COMMUNICATION

Preparation of metal oxide thin films from organic-additive-free aqueous solutions by low-speed dip-coating†

H. Uchiyama,* T. Ito, R. Sasaki and H. Kozuka

Here we propose a novel coating technique with low-speed dip-coating for preparing metal oxide thin films from organic-additive-free aqueous solutions, where the film formation on the substrate is achieved *via* an evaporation-driven deposition during dip-coating of extremely low substrate withdrawal speeds below 1.0 cm min^{-1} in a thermostatic oven at 25–60 °C. Transparent, crack-free SnO$_2$ and TiO$_2$ precursor films were obtained from SnCl$_4$ and TiOSO$_4$ aqueous solutions, respectively, by low-speed dip-coating. The precursor films thus obtained were crystallized to SnO$_2$ and TiO$_2$ films by the heat treatment at 700 °C for 10 min in air.

The sol–gel coating process is widely used for preparing metal oxide films, where precursor solutions are usually produced through the hydrolysis and condensation reactions of metal alkoxides.[1,2] Since metal alkoxides are hydrophobic and immiscible with water, alcohols are used as co-solvents for alkoxides and water. However, alcohols are volatile, inflammable, and hence not favorable solvents to be handled in industries. Therefore, industries strongly demand the replacement of alkoxide-derived precursor solutions by manageable ones.

Recently, aqueous solutions of metal salts are receiving attention as environmentally friendly precursors for metal oxide materials in industrial fields, because water is not inflammable and toxic, and has a lower volatility. However, water has much higher surface tension (72 mN m^{-1}) than alcohols (20–30 mN m^{-1}), and thus many substrates such as glasses, ceramics and metals would show poor wettability by aqueous solutions, inhibiting the homogeneous film formation on the substrates. In order to modify the low wettability, coating methods assisted by organic polymers have been suggested by many researchers. The authors previously reported that the wettability of substrates and the film formation

ability are greatly improved by the addition of organic polymers with amide groups such as poly(vinylpyrrolidone) (PVP), poly(vinylacetamide) and poly(acrylamide) into aqueous solutions of metal salts, where transparent and homogeneous TiO$_2$ and ZrO$_2$ thin films could be prepared from aqueous solutions of Ti(SO$_4$)$_2$ and ZrOCl$_2$, respectively, by dip-coating.[3] Jia *et al.* suggested a polymer-assisted deposition (PAD) method, where the addition of organic polymers such as poly(ethyleneimine) (PEI) with ethylenediaminetetraacetic acid (EDTA) prevents the metal ions from engaging in unwanted chemical reactions, and maintains the desired viscosity of solutions for controlling film thickness, resulting in the deposition of metal oxide films from aqueous solutions.[4–13] These synthetic routes assisted by organic polymers would allow us to achieve many kinds of metal oxide films from aqueous solutions of metal salts.

In this work, we propose a novel coating technique with low-speed dip-coating for preparing metal oxide films from organic-additive-free aqueous solutions. Previously, Faustini *et al.* investigated the deposition of sol–gel-derived metal oxide films by dip-coating at extremely low substrate speeds below 1.0 cm min^{-1}.[14–17] During the low-speed dip-coating, the solvents evaporate from the edge of the meniscus, where the deposition of the solutes locally progresses. Then, the evaporation-driven deposition during dip-coating would hinder aqueous solutions with high surface tension from gathering together to form droplets, allowing the film formation on the substrate. Krins *et al.* achieved the preparation of mesoporous anatase TiO$_2$ films from aqueous solutions containing TiCl$_4$, H$_2$O and an organic block copolymer template (F127) with low-speed dip-coating.[17] However, the preparation of metal oxide thin films from organic-additive-free aqueous solutions by low-speed dip-coating has not been investigated so far. Here, we focused on the low-speed dip-coating as a coating technique for organic-additive-free aqueous solutions, preparing SnO$_2$ and TiO$_2$ films from SnCl$_4$ and TiOSO$_4$ aqueous solutions, respectively. The coating technique accompanied by the evaporation-driven deposition would enable a synthetic route for metal oxide thin films from simple solutions containing only water and metal

Department of Chemistry and Materials Engineering, Kansai University, 3-3-35 Yamate-cho, Suita, 564-8680, Japan. E-mail: h_uchi@kansai-u.ac.jp; Fax: +81-6-6388-8797; Tel: +81-6-6368-1121 ext. 5638

† Electronic supplementary information (ESI) available. See DOI: 10.1039/c4ra16810k

salts without organic additives, providing a low-cost and resource-saving coating process. Since the evaporation-driven deposition would be influenced by the substrate withdrawal speeds and the coating temperatures (*i.e.*, the temperature of substrates, solutions and atmosphere), we investigated the effect of those parameters on the film formation during low-speed dip-coating.

1.4 g of $SnCl_4 \cdot 5H_2O$ (Wako Pure Chemical Industries, Osaka, Japan) and 4.0 g of $TiOSO_4 \cdot xH_2SO_4 \cdot xH_2O$ (Sigma-Aldrich, Co., St. Louis, USA) (the content of $TiOSO_4$ was examined to be *ca.* 69 wt%) were added and dissolved in 40 and 50 cm^3 of purified water, respectively, under stirring at room temperature, resulting in transparent solutions of $[SnCl_4 \cdot 5H_2O] = 0.10$ M and $[TiOSO_4] = 0.35$ M. After stirring at room temperature for 1 h, the solutions served as coating solutions.

Low-speed dip-coating was performed using a dip-coater (Portable Dip Coater DT-0001, SDI, Kyoto, Japan) in a thermostatic oven. Precursor films were deposited on soda-lime glass (26 mm × 38 mm × 1.0 mm) and silica glass substrates (20 mm × 40 mm × 0.85 mm) by dip-coating, where the substrates were withdrawn at 0.05–1.00 cm min^{-1}. The coating temperature, *i.e.*, the temperature of substrates, solutions and atmosphere, was kept at 25–60 °C, where the solutions and substrates were heated at the prescribed temperature for 30 min in the thermostatic oven before the dip-coating. SnO_2 and TiO_2 films were obtained by the heat treatment of the precursor films deposited on silica substrates. The heat treatment was performed at 700 °C for 10 min in air, where the precursor films were directly transferred to an electric furnace held at 700 °C. The dip-coating and the heat treatment were performed one- and three-times, and the resultant films were used as samples.

The microstructure of the thin film samples was observed using a field emission scanning electron microscope (FE-SEM) (Model JSM-6500F, JEOL, Tokyo, Japan). The crystalline phases were identified by X-ray diffraction (XRD) measurement by ordinary $2\theta/\theta$ mode using an X-ray diffractometer (Model Rint 2550V, Rigaku, Tokyo, Japan) with $CuK\alpha$ radiation operated at 40 kV and 300 mA. Infrared (IR) absorption spectra were measured with a Fourier transform infrared (FTIR) spectrophotometer (FT/IR-410, Jasco, Tokyo, Japan). Optical transmission spectra were measured on the film samples using an optical spectrometer (V-570, JASCO, Tokyo, Japan), where a silica glass substrate was used as the reference. Film thickness was measured using a contact probe surface profilometer (SE-3500K31, Kosaka Laboratory, Tokyo, Japan). A part of the thin film was scraped off with a surgical knife immediately after the film deposition, and the level difference between the coated part and the scraped part was measured after drying and heat treatment. The thickness was measured for the precursor and heat-treated films deposited on soda-lime glass and silica substrates, respectively.

SnO_2 precursor films were obtained from the aqueous solution of $[SnCl_4 \cdot 5H_2O] = 0.10$ M with one-time dip-coating at 0.05–0.50 cm min^{-1} in a thermostatic oven at 25–60 °C, and then heated at 700 °C for 10 min in air. Table 1 shows the thickness and appearance of the precursor and heat-treated films obtained from the $SnCl_4$ aqueous solution. Film

formation was not visually confirmed over 0.20 and 0.50 cm min^{-1} at coating temperature of 25 and 40–60 °C, respectively. On the other hand, formation of precursor films on the whole substrates was observed below 0.10 and 0.30 cm min^{-1} at coating temperatures of 25 and 40–60 °C, respectively. The thickness of the precursor films increased with decreasing substrate withdrawal speed and with increasing coating temperature, resulting in the cracking of films below 0.10 cm min^{-1} irrespective of coating temperature. Crack-free precursor films below 40 nm in thickness were obtained between 0.20–0.30 cm min^{-1} at 40–60 °C, where cracks were not observed even after the heat treatment.

The film formation on the substrate was also confirmed by the IR absorption measurement of the SnO_2 precursor films. Fig. 1 shows the IR absorption spectra of the precursor films prepared from the $SnCl_4$ aqueous solution at 0.05–0.30 cm min^{-1} in a thermostatic oven at 25 °C. The absorption bands at around 550, 680, 1600, and 3400 cm^{-1} were detected for the film samples deposited below 0.20 cm min^{-1}. The broad bands at 3400 and 1600 cm^{-1} are assigned to the stretching vibrations of O–H and the bending vibrations of adsorbed H_2O, respectively. The absorption bands at 550 and 680 cm^{-1} may be the symmetric and asymmetric stretching vibrations of Sn–O–Sn bonds.[18–20] These absorption peaks attributed to O–H groups and Sn–O–Sn bonds suggest the deposition of $Sn(OH)_4$ on the substrates. $Sn(OH)_4$ films could be produced from the $SnCl_4$ aqueous solution *via* an evaporation-driven deposition at the meniscus, because $Sn(OH)_4$ is a thermodynamically stable solid phase in a wide range of pH (pH 0–11) in Sn–Cl–H_2O system at 298 K.[21] The peak intensity of Sn–O–Sn bonds increased with decreasing substrate withdrawal speeds, which agreed with the results of the appearance and the film thickness (Table 1). Although Sn–O–Sn vibrations were slightly detected for the samples obtained at 0.20 cm min^{-1} in a thermostatic oven at 25 °C, the precursor films were not formed on the whole substrate (Table 1).

SnO_2 precursor films prepared with one- and three-times dip-coating at 0.20 cm min^{-1} in a thermostatic oven at 60 °C were heat-treated at 700 °C for 10 min in air to obtain crack-free SnO_2 films. The SnO_2 precursor film prepared with one-time dip-coating had flat and smooth surface (ESI Fig. S1a and b†), and had no diffraction peaks in the XRD pattern (ESI Fig. S1c†). Fig. 2 shows the XRD patterns of the heat-treated SnO_2 films. The diffraction peaks attributed to rutile SnO_2 phase were not observed for the heat-treated SnO_2 films prepared with one-time coating, which could be caused by the smaller thickness (*ca.* 40 nm) (Table 1). On the other hand, rutile SnO_2 phase was detected for the three-times coating films with larger thickness. Fig. 3 shows the optical micrograph, SEM image and UV-vis transmission spectrum of the SnO_2 film prepared with three-times dip-coating. The SnO_2 film was found to be crack-free and transparent (Fig. 3a), and to consist of small grains below 50 nm in size (Fig. 3b). High transmittance over 80% in the visible range of 400–800 nm was confirmed for the SnO_2 film (Fig. 3c).

We also attempted the preparation of TiO_2 films from the $TiOSO_4$ aqueous solution with low-speed dip-coating. Precursor films were prepared from the aqueous solution of $[TiOSO_4] =$

Table 1 Thickness and appearance of the precursor and heat-treated films prepared from $SnCl_4$ and $TiOSO_4$ aqueous solutions with one-time dip-coating

Film	Coating temperature/°C	Substrate withdrawal speed/cm min^{-1}	Film formation	Precursor films		Heat-treated films	
				Thickness/nm	Cracking	Thickness/nm	Cracking
SnO_2	25	0.05	Yes	102 ± 34	Yes	43 ± 12	Yes
		0.10	Yes	39 ± 22	Yes	22 ± 5	Yes
		0.20	No	—	—	—	—
		0.30	No	—	—	—	—
		0.50	No	—	—	—	—
	40	0.05	Yes	172 ± 12	Yes	126 ± 31	Yes
		0.10	Yes	76 ± 13	Yes	57 ± 18	Yes
		0.20	Yes	28 ± 17	No	21 ± 4	No
		0.30	Yes	12 ± 17	No	13 ± 2	No
		0.50	No	—	—	—	—
	60	0.05	Yes	290 ± 44	Yes	284 ± 29	Yes
		0.10	Yes	167 ± 14	Yes	90 ± 11	Yes
		0.20	Yes	39 ± 16	No	37 ± 20	No
		0.30	Yes	30 ± 10	No	17 ± 8	No
		0.50	No	—	—	—	—
TiO_2	40	0.05	Yes	620 ± 104	Yes	724 ± 54	Yes
		0.10	Yes	329 ± 18	Yes	329 ± 23	Yes
		0.20	Yes	96 ± 11	No	64 ± 11	No
		0.30	Yes	120 ± 28	No	66 ± 17	No
		0.50	Yes	96 ± 15	No	58 ± 15	No
		1.00	No	—	—	—	—
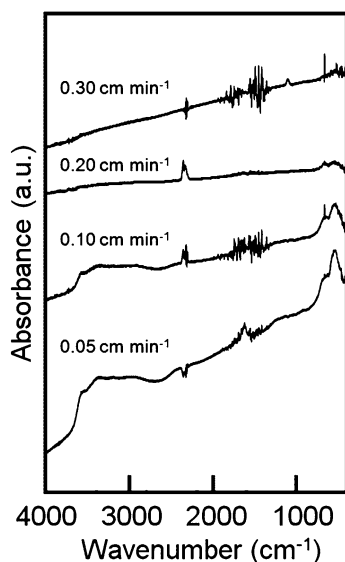
Fig. 1 IR absorption spectra of the SnO_2 precursor films prepared from the aqueous solution of $[SnCl_4 \cdot 5H_2O] = 0.10$ M at 0.05–0.30 cm min^{-1} in a thermostatic oven at 25 °C.

Fig. 2 XRD patterns of the heat-treated SnO_2 films prepared with one- and three-times dip-coating at 0.20 cm min^{-1} in a thermostatic oven at 60 °C.

0.35 M with one-time dip-coating at 0.05–1.00 cm min^{-1} in a thermostatic oven at 40 °C, and then heated at 700 °C for 10 min in air. Film formation was observed with decreasing substrate withdrawal speeds (Table 1), where crack-free precursor and heat-treated films were obtained between 0.20–0.50 cm min^{-1} (Table 1 and ESI Fig. S2†). The heat-treated TiO_2 films prepared with one- and three-times dip-coating at 0.20 cm min^{-1} exhibited the diffraction peaks attributed to anatase TiO_2 phase,
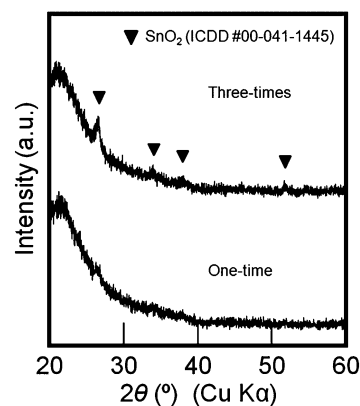
where the peak intensity increased with repeating dip-coating (ESI Fig. S3†).

The film formation from organic-additive-free aqueous solutions was achieved with decreasing substrate withdrawal speed and with increasing coating temperature (Table 1), which could be attributed to the evaporation-driven deposition at the meniscus. The schematic illustration of the evaporation-driven deposition at the meniscus during low-speed dip-coating is shown in Fig. 4. During the dip-coating of extremely low substrate speeds below 1.0 cm min^{-1}, the solvents evaporate from the edge of the meniscus, and then the film deposition locally progresses there.[14–17,22–24] In the present case, lower substrate withdrawal speeds and higher coating temperatures
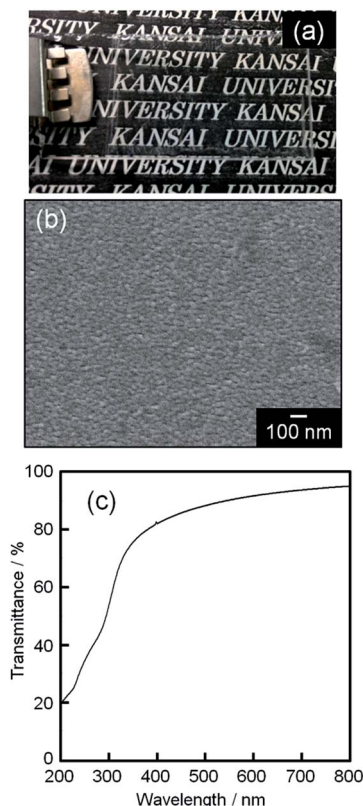
Fig. 3 Optical micrograph (a), SEM image (b) and UV-vis absorption spectrum (c) of the heat-treated SnO_2 films prepared with three-times dip-coating at 0.20 cm min^{-1} in a thermostatic oven at 60 °C.
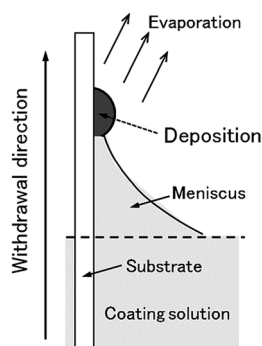

Fig. 4 Schematic illustration of the evaporation-driven deposition at the meniscus.

could progress the evaporation-driven deposition at the meniscus, resulting in the film formation on the substrate during the dip-coating. However, an excessive deposition of precursor films provided larger thickness, involving the cracking of films (Table 1). Thus, the homogeneous film formation from aqueous solutions requires moderate substrate withdrawal speed and solvent evaporation rate.

The coating technique proposed here can be carried out for metal oxides other than SnO_2 and TiO_2 if aqueous solutions containing meal ions as coating solutions can be made. The

low-speed dip-coating would allow any kinds of metal oxide thin films to be obtained from organic-additive-free aqueous solutions, leading to the development of a low-cost and resource-saving coating process.

References

1 H. Dislich, *Angew. Chem., Int. Ed.*, 1971, **10**, 363–370.
2 I. Strawbridge and P. F. James, *J. Non-Cryst. Solids*, 1986, **86**, 381–393.
3 H. Kozuka and T. Kishimoto, *Chem. Lett.*, 2001, 1150–1151.
4 M. Jain, E. Bauer, F. Ronning, M. F. Hundley, L. Civale, H. Wang, B. Malorov, A. K. Burrell, T. M. McClesky, S. R. Foltyn, R. F. DePaula and Q. Jia, *J. Am. Ceram. Soc.*, 2008, **91**, 1858–1863.
5 M. Jain, P. Shukla, Y. Li, M. F. Hundley, H. Wang, S. R. Foltyn, A. K. Burrell, T. M. McCleskey and Q. Jia, *Adv. Mater.*, 2006, **18**, 2695–2698.
6 Q. X. Jia, T. M. McCleskey, A. K. Burrell, Y. Lin, G. E. Collis, H. Wang, A. D. Q. Li and S. R. Foltyn, *Nat. Mater.*, 2004, **3**, 529–532.
7 Q. Lin, Y. Xu, E. Fu, S. Baber, Z. Bao, L. Yu, S. Deng, J. Kundu, J. Hollingsworth, E. Bauer, T. M. McCleskey, A. K. Burrell, Q. Jia and H. Luo, *J. Mater. Chem.*, 2012, **22**, 5835–5839.
8 Y. Lin, J. S. Lee, H. Wang, Y. Li, S. R. Foltyn, Q. X. Jia, G. E. Collis, A. K. Burrell and T. M. McCleskey, *Appl. Phys. Lett.*, 2004, **85**, 5007–5009.
9 Y. Lin, H. Wang, M. E. Hawley, S. R. Foltyn, Q. X. Jia, G. E. Collis, A. K. Burrell and T. M. McCleskey, *Appl. Phys. Lett.*, 2004, **85**, 3426–3428.
10 H. Luo, H. Yang, S. A. Bally, O. Ugurlu, M. Jain, M. E. Hawley, T. M. McCleskey, A. K. Burrell, E. Bauer, L. Civale, T. G. Holesinger and Q. Jia, *J. Am. Chem. Soc.*, 2007, **129**, 14132–14133.
11 H. M. Luo, M. Jain, S. A. Baily, T. M. McCleskey, A. K. Burrell, E. Bauer, R. F. DePaula, P. C. Dowden, L. Civale and Q. X. Jia, *J. Phys. Chem. B*, 2007, **111**, 7497–7500.
12 T. M. McCleskey, P. Shi, E. Bauer, M. J. Highland, J. A. Eastman, Z. X. Bi, P. H. Fuoss, P. M. Baldo, W. Ren, B. L. Scott, A. K. Burrell and Q. X. Jia, *Chem. Soc. Rev.*, 2014, **43**, 2141–2146.
13 G. F. Zou, J. Zhao, H. M. Luo, T. M. McCleskey, A. K. Burrell and Q. X. Jia, *Chem. Soc. Rev.*, 2013, **42**, 439–449.
14 M. Faustini, C. Boissiere, L. Nicole and D. Grosso, *Chem. Mater.*, 2014, **26**, 709–723.
15 M. Faustini, B. Louis, P. A. Albouy, M. Kuemmel and D. Grosso, *J. Phys. Chem. C*, 2010, **114**, 7637–7645.
16 D. Grosso, *J. Mater. Chem.*, 2011, **21**, 17033–17038.
17 N. Krins, M. Faustini, B. Louis and D. Grosso, *Chem. Mater.*, 2010, **22**, 6218–6220.
18 H. A. Avila and J. E. Rodriguez-Paez, *J. Non-Cryst. Solids*, 2009, **355**, 885–890.
19 J. Jouhannaud, J. Rossignol and D. Stuerga, *J. Solid State Chem.*, 2008, **181**, 1439–1444.
20 H. Uchiyama, Y. Shirai and H. Kozuka, *J. Cryst. Growth*, 2011, **319**, 70–78.

21 G. H. Kelsal and F. P. Gudyanga, *J. Electroanal. Chem. Interfacial Electrochem.*, 1990, **280**, 267–282.

22 H. Uchiyama, M. Hayashi and H. Kozuka, *RSC Adv.*, 2012, **2**, 467–473.

23 H. Uchiyama, R. Sasaki and H. Kozuka, *Colloids Surf., A*, 2014, **453**, 1–6.

24 H. Uchiyama, D. Shimaoka and H. Kozuka, *Soft Matter*, 2012, **8**, 11318–11322.